11th International Symposium on Turbulence and Shear Flow Phenomena (TSFP11)
Southampton, UK, July 30 to August 2, 2019

INVESTIGATION OF THE ENERGY CARRYING OUTER LAYER STRUCTURES IN ADVERSE PRESSURE GRADIENT FLOWS

Taygun Recep Gungor
Faculty of Aeronautics and Astronautics
Istanbul Technical University
34469, Istanbul, Turkey
taygun.gungor@itu.edu.tr

Ayse Gul Gungor
Faculty of Aeronautics and Astronautics
Istanbul Technical University
34469, Istanbul, Turkey
ayse.gungor@itu.edu.tr

Yvan Maciel
Department of Mechanical Engineering
Universite Laval
Quebec City, QC, G1V 0A6 Canada
yvan.maciel@gmc.ulaval.ca

Mark Phil Simens
School of Aeronautics
Universidad Politécnica de Madrid
28040 Madrid, Spain
mark@torroja.dmt.upm.es

ABSTRACT

Spatio-temporal energy spectra are analyzed from a direct numerical simulation of a non-equilibrium adverse pressure gradient (APG) turbulent boundary layer (TBL) spanning Re_θ=1500-8200 and shape factor $H = 1.4 - 3$. The temporal data at two streamwise positions corresponding to small ($H = 1.6$) and large ($H = 2.5$) velocity defects are used to obtain the spatio-temporal spectra. The increase in the mean velocity defect has several effects on the energy carrying outer layer structures. The turbulent activity in the inner layer is attenuated. The energy moves away from the wall to the outer layer. The streamwise and spanwise wavelengths of the energy carrying outer layer structures decrease with increasing velocity defect.

INTRODUCTION

A turbulent boundary layer subjected to an APG develops momentum deficit that substantially alters the nature of the flow. In canonical flows such as zero pressure gradient (ZPG) TBLs or channel flows, the turbulent activity is primarily in the near-wall region. In contrast to canonical flows, significant turbulent production exists in the outer layer (Skåre & Krogstad, 1994; Na & Moin, 1998). Maciel *et al.* (2017*a*) showed that sweeps and ejections found in APG TBLs are encountered more frequently and are stronger in the outer layer than in the near-wall region. Also, Maciel *et al.* (2018) demonstrated that turbulent kinetic energy production peaks in the outer layer in APG TBLs. These findings indicate the importance of the outer layer in APG TBLs and highlight the main distinction between APG TBLs and canonical flows.

Several attempts have been made to identify the characteristics of the structures in APG TBLs. Krogstad & Skåre (1995), as one of the earlier studies, demonstrated that the streamwise correlation length is reduced due to the effect of APG for an equilibrium TBL. Rahgozar & Maciel (2011) reported that the frequency of appearance and length of the streaky u-structures are affected by the APG in their experimental study where three APG TBLs and one ZPG TBL were compared. Lee & Sung (2009) examined two TBLs, mild APG and ZPG TBL, and found that the number of low-speed streaks increases and their length gets shorter in the outer region when there is a velocity defect. Maciel *et al.* (2017*b*) examined a DNS database of a strongly non-equilibrium APG TBL with a very thin separation bubble. They reported an increase in the number of the sweeps and ejections in the outer layer and a decrease in the length of the *u* structures, which are less streaky than their ZPG TBL counterparts.

In terms of the kinetic energy carried by the structures, Monty *et al.* (2011) reported that large scale structures in the outer layer are energized when an APG is present by experimentally examining ZPG and APG TBLs. Harun *et al.* (2013) investigated favorable pressure gradient (FPG), ZPG and APG TBLs by analyzing the premultiplied streamwise velocity spectra to understand changes in the characteristics of the large scale structures under the effect of different pressure gradients. They found that the energy in the outer layer increases in APG TBLs when the energy is normalized using the friction velocity (the level of all Reynolds stress components increases everywhere when normalizing with the friction velocity). Also, the streamwise wavelength that the energy peaks at is around 3 boundary layer thickness (δ) in APG TBLs, which is smaller than the ones found in ZPG and FPG TBLs. Lee (2017) also examined a ZPG TBL and three equilibrium APG TBLs by analyzing the spanwise energy spectra and streamwise correlations of the streamwise velocity. He showed that large-scale structures in the log layer are strongly affected by the pressure gradient. In the case of mild APG, the streamwise length scales are longer than the ones in the ZPG TBL, but for the moderate and strong APG cases they are reduced in the log layer. As Harun *et al.* (2013) had done before, he demonstrated that the structures in the outer layer become stronger as the APG increases, but it is important to note that he also normalized energy with the friction velocity. Like in Harun *et al.* (2013) a second peak above the log layer emerges in the premultiplied energy spectra indicating the structures in the outer

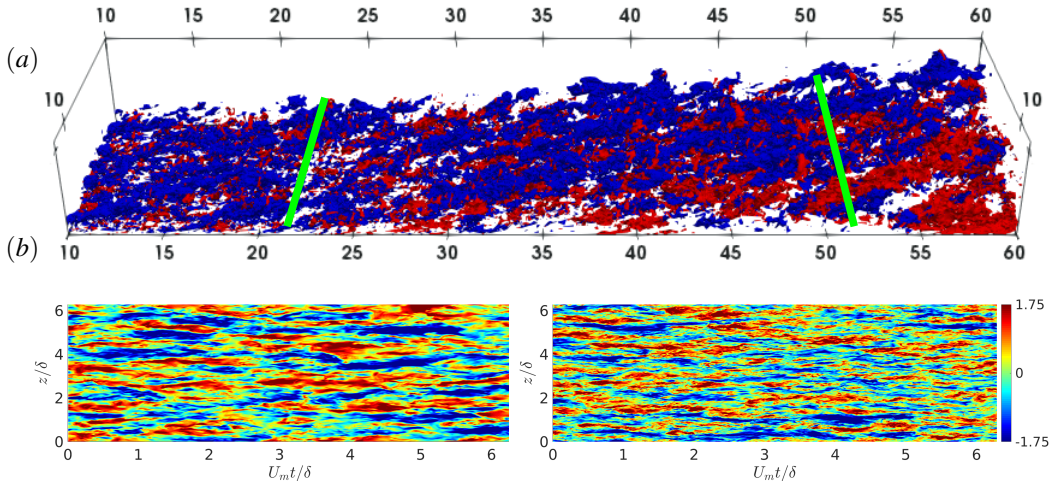

Figure 1. (a) Isosurfaces of the instantaneous streamwise velocity fluctuations normalized with the local rms (σ) of the streamwise velocity. $u = 1.75\sigma$ (red) and $u = -1.75\sigma$ (blue). Green lines indicate the streamwise location of the probes collecting the temporal data. The axes are normalized with inlet δ. (b) Spatio-temporal evolution of the streamwise velocity fluctuations at $H = 1.6$ (left) and 2.5 (right) at $y/\delta = 0.5$. The temporal data are converted into spatial data using the local mean velocity as the convective velocity.

layer carry a considerable amount of energy.

The objective of this study is to investigate the characteristics of the energetic structures found in the outer layer of a non equilibrium APG TBL evolving from small to very large velocity deficit using spatio-temporal spectra. The wavelengths and energy distribution of the structures in the wall-normal direction are examined through premultiplied energy spectra. Some comparisons with the ZPG TBL of Sillero *et al.* (2014) are made.

METHODOLOGY

The present study uses a direct numerical simulation (DNS) dataset of a non-equilibrium TBL subjected to a strong APG that leads to an increasing mean velocity deficit. The flow evolves from a ZPG TBL to an APG TBL near separation. The DNS was performed with a box domain over a no-slip smooth wall, with spanwise periodicity and streamwise non-periodic inflow and outflow. The momentum thickness based on Reynolds number (Re_θ) spans between 1500-8200 and the shape factor (H) increases from 1.4 to 3.0. The computational box dimensions are $(L_x, L_y, L_z)/\theta_{mid} = 151, 29, 42$, where θ_{mid} is taken at the middle of the box, corresponding to N_x, N_y, N_z = $4609 \times 736 \times 1920$ grid points.

The energy carrying structures in the outer layer are explored by analyzing the spatio-temporal spectra. The temporal data are available at four streamwise positions corresponding to $H = 1.6$, 2.0, 2.5 and 2.8. At all streamwise positions, the temporal data are stored for the whole wall normal direction. Taylor's frozen turbulence hypothesis based on the local mean velocity has been employed to transform the temporal data into spatial data in the streamwise direction.

RESULTS

Figure 1(a) presents the spatial development of the low- and high-speed streaks subjected to a strong APG. The streaks rapidly grow in size along the streamwise direction. The near-wall streaks that are numerous in the low defect region, tend to disappear in the large defect zone and become more disorganized. The spatio-temporal evolution of the streaks in the outer layer ($y/\delta = 0.5$) are shown in figure 1(b) at two positions of small ($H = 1.6$) and large mean velocity defects ($H = 2.5$). Very long low-speed streaks are encountered in both flow regions, but they appear to be narrower in the large velocity deficit case.

The energy carrying outer layer structures are studied by analyzing the energy spectra. The premultiplied energy spectra of the streamwise velocity ($k_x \phi_{uu,x}$) as a function of streamwise wavelength (λ_x/δ) and wall normal distance y/δ are presented in figure 2 at two streamwise positions, corresponding to small ($H = 1.6$) and large ($H = 2.5$) mean velocity defects. There are two peaks in the energy spectra of the small velocity defect region, one in the inner layer and one in the outer layer. It is well known that intense turbulence activity is present in the near-wall region of canonical flows such as ZPG TBLs or channel flows. For such flows, an outer peak in the premultiplied spectra of canonical flows emerges only at high Reynolds numbers (Hutchins & Marusic, 2007). Therefore, the outer peak in the small velocity defect region of the present flow is associated with outer layer turbulent activity that occurs due to the velocity defect, possibly because of the strong mean shear in the outer region. In the large velocity defect region, the inner peak completely vanishes, as shown in figure 2(b). The energy-carrying structures are dominantly found in the outer layer of the boundary layer. Furthermore, the shape of both spectra is significantly different. This shows that the defect affects not only the most energetic structures, but also the other ones having less turbulent energy.

Harun *et al.* (2013) compared premultiplied streamwise energy spectra of FPG, ZPG and APG TBLs. Their APG TBL corresponds to a mild APG case with characteristics similar to the present TBL at $H = 1.6$. There are two peaks in the spectra of their APG TBL as in present small velocity defect case. The outer maxima of the energy spectra of their APG TBL is located around $y/\delta = 0.1 - 0.3$ and $\lambda_x/\delta = 2 - 5$. These results are consistent with the present streamwise spectra for the small velocity deficit case, al-

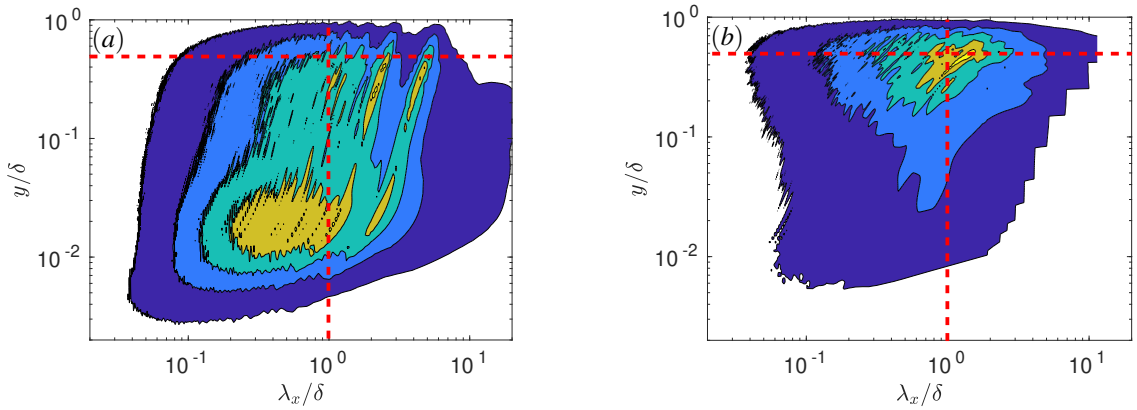

Figure 2. Premultiplied streamwise energy spectra of the streamwise velocity as a function of λ_x/δ and y/δ for two streamwise locations corresponding to small velocity defect, H=1.6, (a) and large velocity defect, H=2.5, (b). The levels are for 0.1, 0.3, 0.5, 0.7 and 0.9 of the maximum of each spectra. Red dashed lines denote $\lambda_x/\delta = 1$ and $y/\delta = 0.5$.

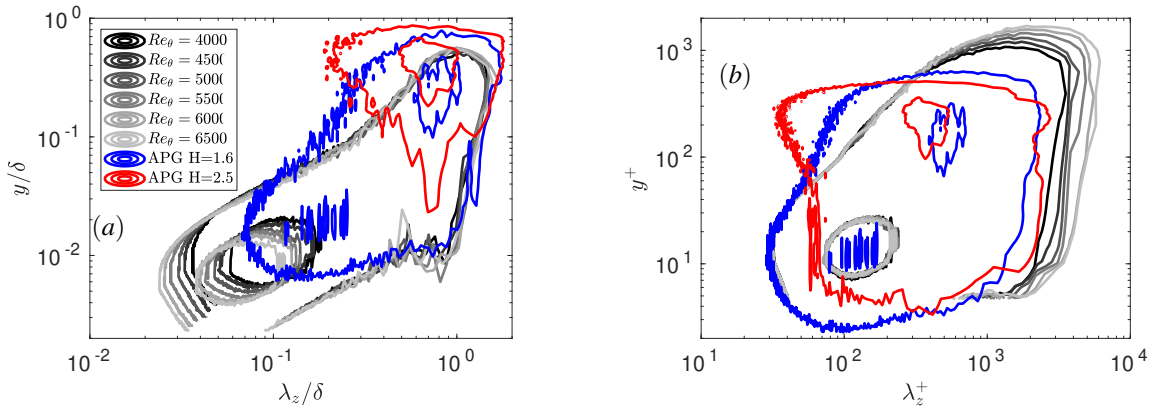

Figure 3. Premultiplied spanwise energy spectra of the streamwise velocity as a function of λ_z and y for the ZPG TBLs of Sillero *et al.* (2014) at different Re_θ (gray lines) and the two streamwise locations of the APG TBL corresponding to $H = 1.6$ (blue line) and 2.5 (red line). The axes are normalized using δ (a) and viscous units (b). The levels are for 0.1 and 0.7 of the maximum of each spectra.

though the latter spectra is not converged enough to determine the precise location of the outer peak.

The premultiplied spanwise spectra ($k_z\phi_{uu,z}$) for the small and large velocity defect of the APG TBL are shown in figure 3 along with the ZPG TBL data of Sillero *et al.* (2014) at several Reynolds numbers. For the APG TBL small and large defect locations, Re_θ is 2850 and 5850, respectively. The spectra axes are scaled by the local δ in figure 3(a) since the focus is on the outer layer structures and by the local viscous units in figure 3(b). When plotted in viscous units, the inner peak of ZPG spectra and low defect APG spectra collapse, as shown in figure 3(b). δ does not scale the wall-normal location and spanwise wavelength (λ_z) of the inner peak of the ZPG data and low defect APG data as expected, since δ is not a proper scale for the inner layer structures. When normalized with δ, the outer contour collapses for the different Re_θ of the ZPG TBLs but not for the APG TBLs. As with the streamwise spectra, the spanwise spectra of APG TBLs exhibit an outer peak and their shape changes with velocity deficit. As the deficit increases, the energy becomes concentrated in the outer region.

Figure 4 displays premultiplied two-dimensional streamwise velocity spectra, $k_x k_z \phi_{uu}$, as a function of λ_x and λ_z at $y/\delta = 0.5$. The three spectra shown are for the same two streamwise positions of the APG TBL as before, and for the ZPG TBL at $Re_\theta = 4857$. In figure 4(a), λ_x and λ_z are scaled by the local δ of each data. The location of the outer peak is not clearly apparent because statistical convergence of the temporal data for $H = 2.5$ has yet to be achieved. As the defect increases the outer contour level (0.1 of the maximum of the energy spectra) moves to the shorter wavelengths. λ_z of the most energetic structures (inner contour levels) of the APG TBLs matches the λ_z of ZPG TBL. In figure 4(b), the Corrsin length scale, L_c, is used to scale the streamwise and spanwise wavelengths. It is defined as $L_c = (\varepsilon/S^3)^{1/2}$ where ε is the dissipation of turbulent kinetic energy and S is the mean shear. It represents the scale of the smallest structures that interact directly with the mean shear. It appears that L_c can be an alternative scale for the size of outer layer structures for different velocity defects.

The size of the less energetic structures tends to follow approximately $\lambda_x \sim \lambda_z^2$ for both ZPG and APG TBLs as it is shown in figure 4 with straight lines. However, this relationship does not hold for the structures carrying most of the energy (the inner contour). λ_x of these structures tends to grow at a higher rate than λ_z^2. Moreover, shapes of the spectra are very similar for the three velocity defect situations. This indicates that the velocity defect does not significantly affect the streamwise-spanwise length ratio of the energy carrying

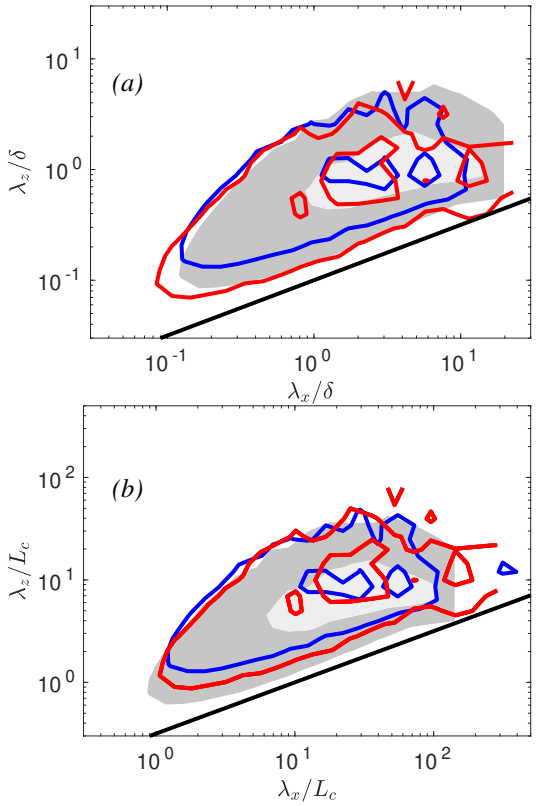

Figure 4. Premultiplied two-dimensional energy spectra of the streamwise velocity as a function of λ_x and λ_z at $y = 0.5\delta$ for the ZPG TBL of Sillero *et al.* (2014) (shaded area) and the two streamwise positions of the APG TBL corresponding to $H = 1.6$ (blue) and 2.5 (red). The straight lines denote $\lambda_x \sim \lambda_z^2$. The axes are normalized using δ (a) and L_c(b). The levels are for 0.1 and 0.5 of the maximum energy of the spectra.

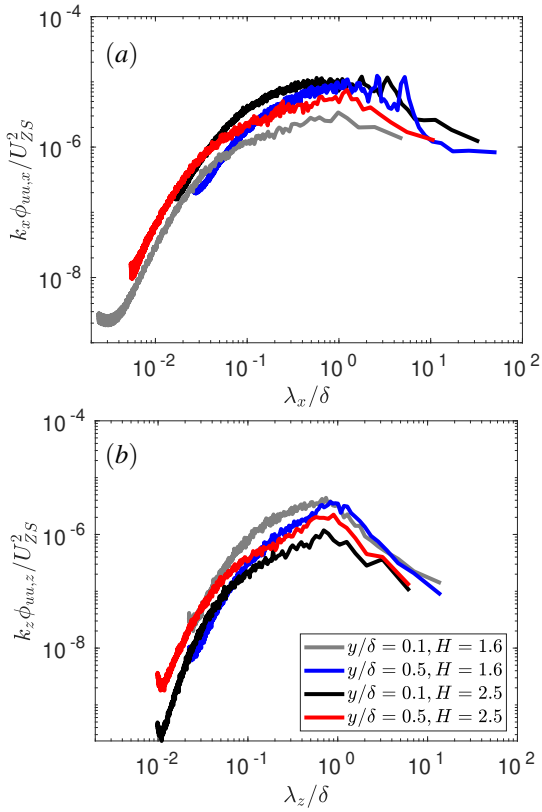

Figure 5. (a) Premultiplied streamwise energy spectra of the streamwise velocity as a function of λ_x. (b) Premultiplied spanwise energy spectra of the streamwise velocity as a function of λ_z. Spectra are displayed for the two streamwise positions at two wall-normal locations corresponding to inner layer ($y/\delta = 0.1$) and outer layer ($y/\delta = 0.5$). Energy and wavelengths are normalized with U_{ZS} and δ, respectively.

structures in the outer layer, although differences do exist and have been discussed before with the one-dimensional spectra. In addition to that, the lack of a linear relationship between the streamwise and spanwise wavelengths shows that the outer layer energetic structures are not self-similar.

In order to compare the energy levels of the two streamwise positions with different velocity defects, the energy is normalized by the Zagarola-Smits velocity scale, U_{ZS}, $U_{ZS} = U_e\delta^*/\delta$, where U_e is the velocity at the boundary layer edge and δ^* is the displacement thickness. The normalized streamwise velocity spectra of the two velocity defects are shown in figure 5 at two wall-normal positions, corresponding to inner layer ($y/\delta = 0.1$) and outer layer ($y/\delta = 0.5$). The energy of the outer layer structures decreases as the velocity defect increases when the spectra are normalized with U_{ZS}. This is consistent with the fact that the streamwise Reynolds normal stresses decrease in the outer region as the defect increases when normalized with U_{ZS}, and so do the other Reynolds stress components and turbulence production and transport (Gungor *et al.*, 2016; Maciel *et al.*, 2018). Note that u_τ does not scale the Reynolds stresses for large velocity defect TBLs. As observed previously, it is clear that while turbulence activity is significantly higher in the inner layer than in the outer layer of the small velocity defect region, the opposite is true for the large velocity defect region. Energy levels of the outer layer and inner layer in the small velocity defect region become very similar at high wavelengths, approximately after λ_x/δ and $\lambda_z/\delta = 1$. In the large velocity defect region, energy of the outer layer structures remains higher than the energy of the inner layer ones through the whole spectrum.

In figure 6, wall-normal distance (y_{max}) and wavelength ($\lambda_{z,max}$) of the maximum of $k_z\phi_{ii,z}$ ($i = u, v$ and w) are illustrated as a function of the shape factor for three components of the velocity for the current case (APG1) along with another APG TBL case (APG2) which is presented by Gungor *et al.* (2016). Results from both APG TBLs coincide very well with each other. Figure 6(a) shows y_{max} normalized with δ. At the very beginning of the domain where $H < 1.6 - 1.7$, the TBLs can be considered as a ZPG TBL because the velocity defect is still very small. As the defect increases, the energetic structures for all velocity components moves further away from the wall. The upward shift ceases when H reaches approximately 2.6. After that point, y_{max}/δ remains constant at 0.5. Figure 6(b) displays $\lambda_{z,max}$ normalized with δ. At the beginning of the domain where the TBLs act like a ZPG TBL, $\lambda_{z,max}/\delta$ is around 0.2-0.4 for all the velocity components. Once H reaches 1.6, $\lambda_{z,max}$ rapidly increases for the streamwise and spanwise components of the velocity. The spanwise wavelengths of the energetic u- and w-structures are similar, around 0.6δ to 0.8δ, while it is shorter for the energetic v-structures, around 0.2δ to 0.4δ. This shows that the outer layer structures be-

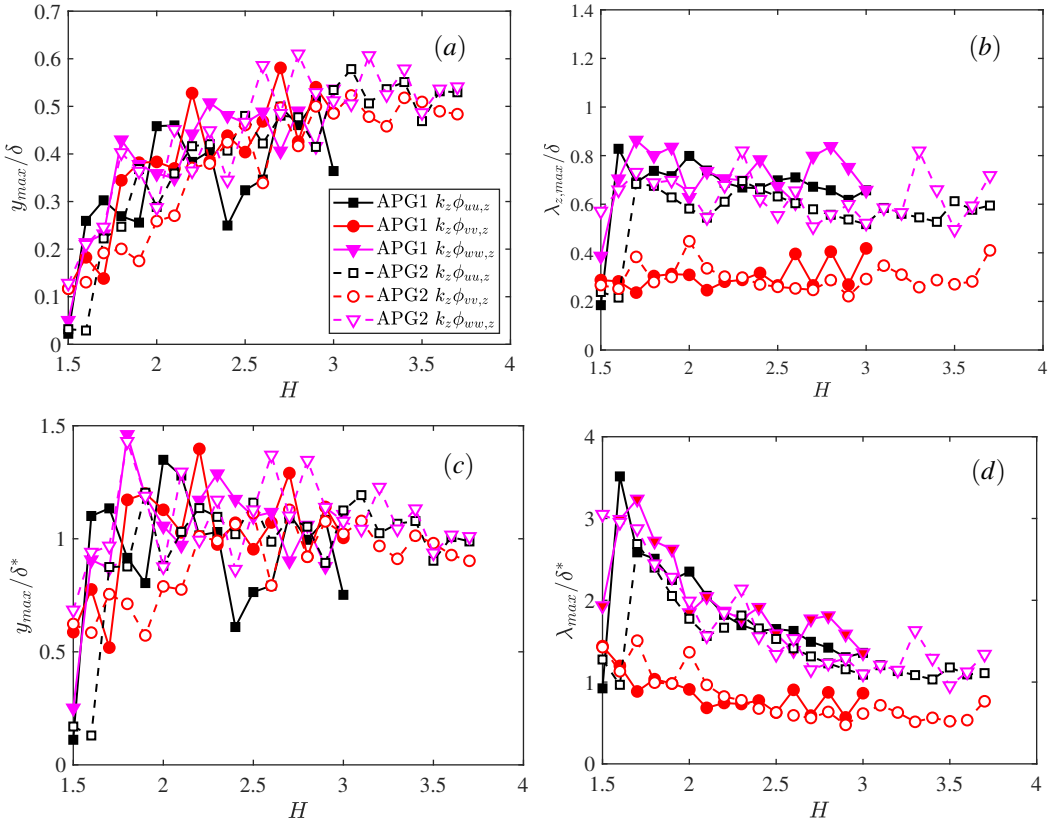

Figure 6. The wall-normal position (y_{max}) and spanwise wavelength ($\lambda_{z,max}$) of the maximum of the premultiplied energy spectra as a function of H for the current case (APG1) and APG of Gungor *et al.* (2016) (APG2). λ_{max} and y_{max} are normalized by the local δ in (a) and (b) and the local δ^* in (c) and (d).

comes dominant and start carrying more energy than the inner layer structures for the streamwise and spanwise components. In figure 6(c) and 6(d), λ_{max} and y_{max} are now normalized with δ^*. The most notable feature is that the wall-normal location of the energetic structures becomes invariant when scaled with δ^* after the defect becomes strong enough ($H > 1.8$). This result is consistent with the findings of Maciel *et al.* (2018), namely that the wall normal position of the maximum Reynolds stresses are around $y/\delta^* = 1$.

Lee (2017) reported spanwise wavelengths, $\lambda_{uu,max}/\delta$ of 0.88, 0.9 and 0.96 and $y_{uu,max}/\delta$ of 0.28, 0.36 and 0.46 for three equilibrium TBL cases with moderate to strong APGs ($H = 1.56, 1.72$ and 1.98, respectively). $\lambda_{uu,max}$ is greater in Lee's study than $\lambda_{uu,max}$ of the current results. The non equilibrium nature of the present flows (increasing velocity defect) might modify the spanwise wavelength of the energetic structures. However, $y_{uu,max}$ is fairly similar in both cases. Kitsios *et al.* (2017) have examined premultiplied spanwise energy spectra of a near-equilibrium APG TBL with a large velocity defect ($H = 2.3 - 2.4$). They found that wall-normal distance and spanwise wavelength of maxima of the premultiplied energy spectra of the streamwise velocity are $1\delta^*$ and $2\delta^*$, respectively. While $y_{uu,max}$ is consistent with the results of the current study, $\lambda_{uu,max}$ of the present cases is smaller than theirs. Again, this difference might originate from the fact that their case is a near-equilibrium one while the present flows are in strong non-equilibrium.

CONCLUSIONS

The energetic outer layer structures of a non-equilibrium APG TBL have been examined through the energy spectra for different velocity defects. The APG TBL has a ZPG-like behavior, especially in the near-wall region, when the defect is small. The energy moves away from the near-wall region to the outer layer with increasing defect. The streamwise wavelength of the energetic structures in the outer layer is attenuated as the velocity defect increases. The spanwise wavelength also diminishes, but not as significantly. Furthermore the relationship between λ_x and λ_z does not seem to be affected significantly by the velocity defect. The spanwise wavelengths of the energetic u- and w-structures are similar, around 0.6δ to 0.8δ. The energetic v-structures have a smaller λ_z of around 0.2δ to 0.4δ.

ACKNOWLEDGMENTS

A.G.G. and T.R.G were supported by Research Fund of the Istanbul Technical University with the project number of MGA-2017-40731. T.R.G and Y.M are supported by NSERC of Canada. Computations of the present data was made possible by a generous grant of computer time from Compute Canada.

REFERENCES

Gungor, A. G., Maciel, Y., Simens, M. P. & Soria, J. 2016 Scaling and statistics of large-defect adverse pressure gradient turbulent boundary layers. *International Journal of Heat and Fluid Flow* **59**, 109–124.

Harun, Z., Monty, J. P., Mathis, R. & Marusic, I. 2013 Pressure gradient effects on the large-scale structure of turbulent boundary layers. *Journal of Fluid Mechanics* **715** (639), 477–498.

Hutchins, N. & Marusic, I. 2007 Evidence of very long meandering features in the logarithmic region of turbulent boundary layers. *Journal of Fluid Mechanics* **579**, 1–28.

Kitsios, V., Sekimoto, A., Atkinson, C., Sillero, J. A., Borrell, G., Gungor, A. G., Jiménez, J. & Soria, J. 2017 Direct numerical simulation of a self-similar adverse pressure gradient turbulent boundary layer at the verge of separation. *Journal of Fluid Mechanics* **829**, 392–419.

Krogstad, P. Å. & Skåre, P. E. 1995 Influence of a strong adverse pressure gradient on the turbulent structure in a boundary layer. *Physics of Fluids* **7** (8), 2014–2024.

Lee, J. H. 2017 Large-scale motions in turbulent boundary layers subjected to adverse pressure gradients. *Journal of Fluid Mechanics* **810**, 323–361.

Lee, J. H. & Sung, H. J. 2009 Structures in turbulent boundary layers subjected to adverse pressure gradients. *Journal of Fluid Mechanics* **639**, 101–131.

Maciel, Y., Gungor, A. G & Simens, M. P. 2017*a* Structural differences between small and large momentum-defect turbulent boundary layers. *International Journal of Heat and Fluid Flow* **67**, 95–110.

Maciel, Y., Simens, M. P & Gungor, A. G. 2017*b* Coherent structures in a non-equilibrium large-velocity-defect turbulent boundary layer. *Flow, Turbulence and Combustion* **98** (1), 1–20.

Maciel, Y., Wei, T., Gungor, A. G & Simens, M. P 2018 Outer scales and parameters of adverse-pressure-gradient turbulent boundary layers. *Journal of Fluid Mechanics* **844**, 5–35.

Monty, J. P., Harun, Z. & Marusic, I. 2011 A parametric study of adverse pressure gradient turbulent boundary layers. *International Journal of Heat and Fluid Flow* **32** (3), 575–585.

Na, Y. & Moin, P. 1998 Direct numerical simulation of a separated turbulent boundary layer. *Journal of Fluid Mechanics* **374**, 379–405.

Rahgozar, S. & Maciel, Y. 2011 Low- and high-speed structures in the outer region of an adverse-pressure-gradient turbulent boundary layer. *Experimental Thermal and Fluid Science* **35** (8), 1575–1587.

Sillero, J. A., Jim'enez, J. & Moser, R. D. 2014 Two-point statistics for turbulent boundary layers and channels at reynolds numbers up to delta 2000. *Physics of Fluids* **26** (10), 105109.

Skåre, P. E. & Krogstad, P. 1994 A turbulent equilibrium boundary layer near separation. *Journal of Fluid Mechanics* **272**, 319–348.